Supplementary Information

Interfacial Effects in Janus HfSSe/SnSSe van der Waals Heterostructure: Synergistic Enhancement of Optical Absorption and Thermoelectric Performance

Ali Shahzad [1], Santunu Purohit [1] and Lin Zhu [1*]

[1]School of Physics and Wuhan National High Magnetic Field Center, Huazhong University of Science and Technology, Wuhan 430074, China

[*]Author to whom correspondence should be addressed: linzh@hust.edu.cn

Section I. Computational Methods

The computational reliability of our first-principles calculations was rigorously verified through systematic convergence tests. First, the plane-wave cutoff energy (ENCUT) and the electronic self-consistency criterion (EDIFF) were tested. Total energy calculations performed with cutoff energies ranging from 400 eV to 500 eV, in conjunction with a stricter convergence criterion of 10^{-6} eV, demonstrated excellent convergence. The maximum energy variation was found to be less than 7.36 meV, confirming that the chosen parameters of ENCUT = 400 eV and EDIFF = 10^{-5} eV are sufficient to yield reliable and well-converged results.

To ensure the accuracy of the calculated optical properties, extensive convergence tests were conducted with respect to several key parameters: the number of empty bands (NBANDS), the k-point sampling mesh, the smearing method, and the plane-wave cutoff energy. The final optical calculations employed ENCUT = 400 eV and Gaussian smearing (ISMEAR = 0) with a width of SIGMA = 0.05 eV. Tests on the number of bands compared NBANDS = 75 and 100, while k-point meshes of 7×7×1 and 9×9×1 were evaluated. The optical absorption spectra showed negligible changes in both peak positions and intensities when NBANDS ≥ 75 and a 9×9×1 k-point mesh was used. Consequently, NBANDS = 75 and a 9×9×1 Γ-centered k-grid were selected for all production calculations of optical properties.

The optical absorption spectra were computed using the GW+Bethe-Salpeter equation (GW+BSE) method to explicitly account for electron-hole (excitonic) interactions, which are crucial for accurately describing the optical response of two-dimensional materials. The computational workflow involved successive steps of structural relaxation, self-consistent field (SCF) calculation, exact diagonalization, GW_0 calculation, and finally the BSE calculation, utilizing the generated WAVECAR and WAVEDER files.

Lattice thermal conductivity (κ_l) was calculated using second- and third-order interatomic force constants (IFCs), computed with 4×4×1 and 3×3×1 supercells respectively. Both calculations used a 3×3×1 k-point mesh and a real-space interaction cutoff radius of 4.6 Å. The phonon Boltzmann transport equation was then solved with the ShengBTE code, using a dense 60×60×1 q-point mesh to ensure κ_l convergence. It should be noted that non-analytical corrections (NACs), involving Born effective charges and the dielectric tensor, were not included in the present lattice dynamics calculations. Although NAC can affect long-wavelength optical phonons in polar materials, their impact on κ_l is typically minimal.

Section II. Figures and Table

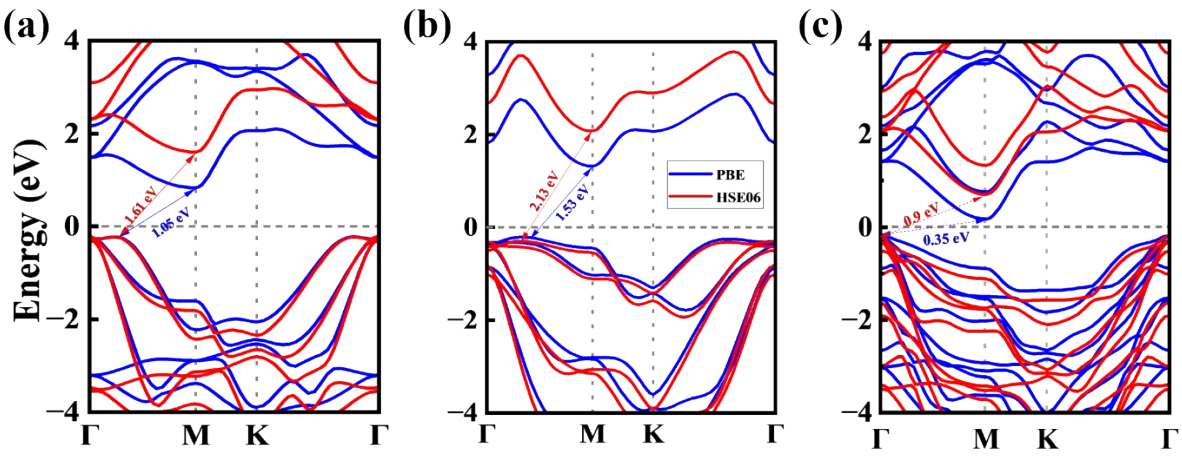

Figure S1. Band structures of HfSSe (a), SnSSe (b) and SnSSe/HfSSe (c) monolayers, calculated using PBE and HSE06. The blue line denotes the PBE calculation, and the red line shows the HSE06 calculation.

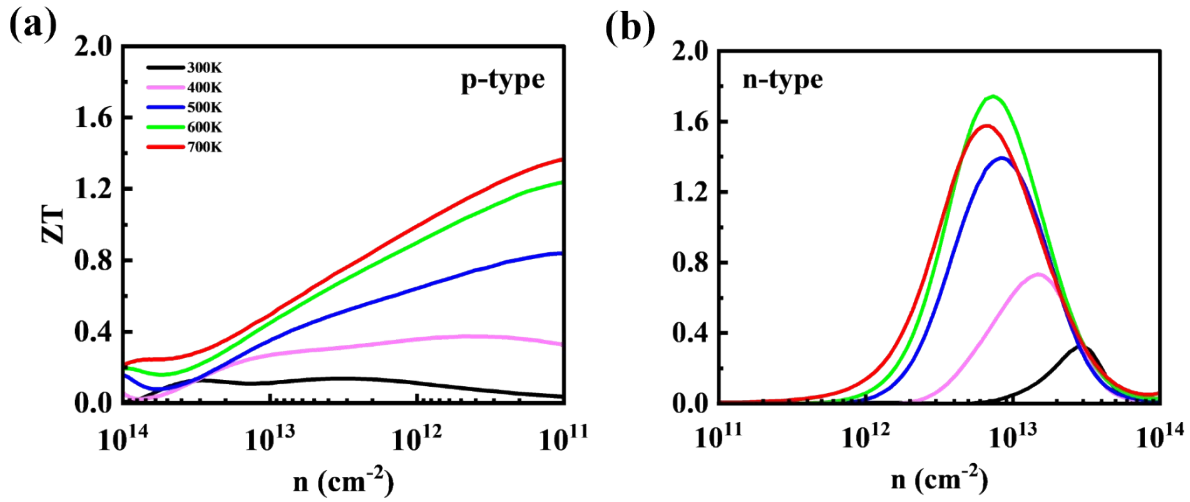

Figure S2. ZT versus carrier concentration for p-type (a) and n-type (b) doping, with a τ value of 10^{-13} s, at different temperatures (300–700 K).

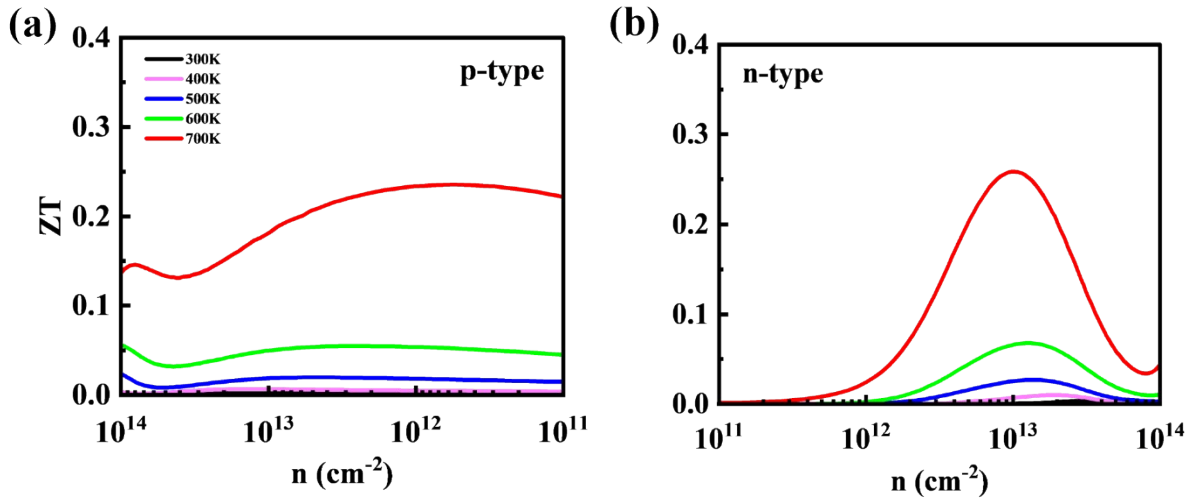

Figure S3. ZT versus carrier concentration for p-type (a) and n-type (b) doping, with a τ value of 10^{-15} s, at different temperatures (300–700 K).

Table S1. Variation of tunneling probability (T_B) with barrier width (W_B) and effective mass (m^*/m_0), demonstrating robust interlayer tunneling behavior.

W_B (Å)	$m*/m_0$	T_B
0.79	0.2	59.48
0.79	0.5	43.98
0.79	1.0	31.29
0.89	0.2	55.69
0.89	0.5	39.63
0.89	1.0	27.01
0.99	0.2	52.15
0.99	0.5	35.72
0.99	1.0	23.32